NASA ULI

Safe, Low-Noise Operation of UAM in Urban Canyons via Integration of Gust Outcomes and Trim Optimization

Annual Report, Year 2

Sheryl Grace, PI
Assoc. Prof. Mechanical Engineering
Boston University
617-353-7364
sgrace@bu.edu

POP: Year 2, 8/1/24 - 7/31/25
Submission date: 8/1/2025
Final report: NO

Trustees of Boston University, 1 Silber Way, Boston, MA 02215-1703
UEI: THL6A6JLE1S7

Award Number: 80NSSC23M0057

Executive Summary

This ULI addresses NASA's ULI Strategic Thrust 4: Safe, Quiet, and Affordable Vertical Lift Air Vehicles. The main focus of the proposed research is the development of critical knowledge and prediction methods for addressing a main barrier to the development and adoption of Urban Air Mobility (UAM): *community noise*. The proposed project will enable the development of validated approaches to assist with the design of safe low-noise multirotor vehicles and control strategies for operation in urban settings. The developed methods will facilitate the investigation of potential UAM vertiport locations and flight corridors. The team is made up of researchers from Boston Univ., Embry Riddle Univ., Tuskegee Univ., Virginia Tech and Joby Aviation with educational partner Univ. of Maryland Eastern Shores.

This work supports ARMD's outcome for 2025-2035: New vertical lift configurations and technologies introduced that enable new markets, increase mobility, improve accessibility, and reduce environmental impact. The proposed research targets major outcome risks by improving the aeroacoustic modeling of UAM vehicles subject to environmental disturbances guiding both their future design and operation.

Major goals and objectives

The requirements that UAM be safe like traditional aircraft, closer to carbon neutral than traditional aircraft, and provide vertical take-off and landing (VTOL) have driven designs that use multiple rotors. These vehicles come in a significant variety of configurations. A believed benefit is much quieter vehicles compared to traditional single large-rotor vehicles. However, UAM are expected to operate much closer to population centers on a more continuous basis than traditional aircraft. Furthermore, they will take off and land from rooftops that may be near other taller buildings and then fly in the urban canyon. The overarching objective of this research is to address fundamental knowledge gaps related to performance and noise that are critical for enabling UAM operation in an urban setting. To this end, the following activities are being undertaken to specifically address the following technical challenges:

Overview of accomplishments by technical challenge

TC 1: *The effect of urban flows on UAM performance and noise.*

This is an expansive topic that has been largely unstudied previously. This project adopts a multipronged approach for addressing fundamental knowledge building blocks that support better understanding and prediction capabilities for multirotor vehicles in urban flows. This is a summary of the inquiries in year 2.

- Urban modeling
  - Single building urban flow simulations at different Reynolds numbers and with upstream turbulence.
  - Canonical multibuilding simulations
  - Realistic city simulations with focus on potential vertiport.
  - Disturbance characterization

- Experimental campaign with single Joby prop
  - Continued analysis of the first year test of scaled single Joby prop. Scan of the prop.
  - Implementation of disturbance generator in SMART (Subsonic Modular Anechoic Research Tunnel). PIV measurements taken.
  - Measurements of APC prop downstream of disturbance generator in SMART.
- Mid fidelity modeling
  - CHARM analysis of single Joby.
  - CHARM analysis of SUI.
  - Airfoil tables development and testing.
  - CHARM thickness file testing.
  - Helios-ROAM simulations of Joby prop flying through urban flow.
- High fidelity modeling
  - Continued permeable FWH analysis.
  - Continued single Joby prop simulations.
  - Joby prop with disturbances of various types.

TC 2: *The effect of UAM trim state on performance and noise.*

This TC requires full vehicle performance and noise assessment as well as improved methods for trim determination. Progress was made on algorithm development for use in a trim model.

- SUI quadrotor state and noise database created using CHARM.
- Machine learning type algorithm to utilize database for quick state prediction tested.

TC 3: *The impact of noise as a metric on UAM path planning.*

Path planning and control algorithms that take into consideration noise as an additional metric do not exist, but may prove critical to gain community buy-in for UAM.

- RRT*+CBF planning method that allows for inclusion of noise metric demonstrated in simulation.
- Path planning algorithm tested in lab using small Tello drones.

Products

- A successful outreach workshop was run at Embry Riddle Aeronautical University May 14-16; 18 students were recruited from universities across the country.
- Joby hosted 4 interns during summer of 2025 from the ULI schools
- "Investigation of the Aerodynamic and Acoustic Performance of a Scaled eVTOL Propeller in Axial and Non-Axial Flight," Ryan D. Lundquist, MS Thesis VT, 2025
- "The Interaction of a Transient Forward Axial Disturbance Flow With a Rotor," Zhuorui Li, MS Thesis ERAU, 2025

- “Aeroacoustic Applications to Jets and Rotors,” Michael Marques G., PhD. Thesis ERAU, 2025.
- “Wake Interaction with a Propeller of an Urban Air Mobility,” Hua, J., Afari, S. O., Golubev, V., and Mankbadi, R. R., *AIAA Journal*, 1-15, (2025).
- “Spectral proper orthogonal decomposition analysis of coherent vortical structures in the wake of a rectangular cylinder.” Maleki, Alireza, Reda R. Mankbadi, and Vladimir Golubev. , *Physics of Fluid*s 37, no. 4 (2025).
- “Flow structures near a tall urban air mobility vertiport: a large-eddy simulation study,” Akinlabi E.O., Maleki A., Golubev V., Grace S., Li D.: *Journal of Wind Engineering and Industrial* Aerodynamics - under review 4/2025
- “Assessment of Self-Noise Models using NFAC Measurements of the Joby Aviation Propeller,” Nikos Trembois, Michael Marques, Austin Thai and Jeremy Bain, SciTech, 2025.
- “High Fidelity Simulation of Noise for Wake Interaction With a Propeller,” Hua, J., Afari, S., Golubev, V. V., and Mankbadi, R. R, AIAA SCITECH, 2025
- “High-Fidelity Analysis of Synthetic Turbulence Effects on Vertiport Unsteady Flow Characteristics,” Alireza Maleki, Surabhi Singh and Vladimir Golubev, AIAA SCITECH, 2025.
- “Noise of a Propeller Designed for eVTOL Operations in Forward and Edgewise Flight”, Huang, S., Chaware, S., Lundquist, R., Intaratep, N., and Alexander, W.N., VFS Forum 81.
- ”A Spectral Proper Orthogonal Decomposition Analysis of Turbulent Flow Around a High-Rise Building.” Maleki, A., Golubev, V., Mankbadi, R., AIAA Aviation, 2025.
- “Rozman, A. and Grace, S., Evaluation of Urban-Flow-Informed Gusts on eVTOL Vertiport Approach Acoustics,” AIAA Aviation 2025.
- “Interaction of Edgewise Transient Disturbance with a Propeller. Hua, J., Golubev, V., and Mankbadi, R. R. AIAA Aviation 2025.
- “The Interaction of a Transient Gust Flow with a Rotor,” Li, Z., Hua, J., Salehian, S., Golubev, V. V., Mankbadi, R. R., AIAA Aviation, 2025.
- “Acoustic Characteristics of a Propeller Experiencing Transient Disturbances in Forward and Edgewise Flight Conditions”, Chaware, S., Huang, S., Duong, T., Lundquist, R., Intaratep, N., and Alexander, W.N., AIAA Aviation 2025.

Impact

The findings related to best practices for propeller and multirotor modeling have been disseminated through conference presentations and papers as listed above. The project has increased the knowledge in the rotorcraft field for how mid-fidelity tools work for predicting performance and noise from multirotor vehicles; how high-fidelity tools compare to each other and experiment for performance and noise of single propellers; a best practice method for computing noise of a propeller near a vertiport was developed; first results for propellers reacting to disturbances are now available. Relevant urban flow disturbances that will be encountered near vertiports have been determined based on simulations. A new method of path planning that allows for the inclusion of noise as a parameter has been demonstrated in simulation and in the lab.

The outreach workshop and Joby internships enlarge the pool of people who know about the emerging urban air vehicle market and techniques used to model UAM performance and noise.

Participants and other collaborating organizations

Name	Organization	Rank	Salary mo.	For. Collab	For. Travel
Sheryl Grace	BU	Assoc. Prof.	1.5	N	N
	PI				
Roberto Tron	BU	Assoc. Prof.	0.8	N	Y, ITLY
	Co-I. Controls.				
Dan Li	BU	Assoc. Prof.	0.8	N	Y, JPN, GER, CHIN
	Co-I. Urban flows.				AUST, BELG, ITLY, NL
Emmanuel Akinlabi	BU	Post doc	0.5	N	N
	Urban flows PALM				
Adam Rozman	BU	PhD Student	12	N	N
	High and mid prop sims - Helios, CHARM; BB noise.				
Idris Seidu	BU	PhD Student	9	N	N
	Path planning; JA intern				
Leo (Xinhuan) Sang	BU	PhD Student	7	N	N
	Mutirotor trim				
Nuo Li	BU	PhD Student	1	N	N
	Broadband noise modeling				
Vladimir Golubev	ERAU	Prof.	1	N	Y, RUS, JPN, ITLY, MEX
	Co-I. Urban & propeller sims				PHIL, TRKY, CHIL
Tasos Lyrintzis	ERAU	Prof.	1	N	Y, GRC
	Co-I. Propeller sims				
Reda Mankbadi	ERAU	Prof.	1	N	N
	Co-I. Propeller sims				
Alireza Maleki	ERAU	PhD Student	12	N	N
	Urban flow sims OpenFOAM				
Michael Marques-G.	ERAU	PhD Student	9	N	N
	High and mid prop sims - OpenFOAM, CHARM; BB noise; JA intern				
Jie Hua	ERAU	PhD Student	12	N	N
	High fid prop sims with dist. OpenFOAM				
Zhourui Li	ERAU	MS student	4	N	N
	High fid prop sims with dist. OpenFOAM				
Daniel Maleev	ERAU	MS student	0	N	N
	Prop sims overflow; JA intern				
Jordan Mills	ERAU	MS student	2	N	N
	Prop sims overflow; NASA intern				
Stanley Ossyra	ERAU	PhD student	9	N	N
	Mid prop sims DUST, FLOWUnsteady; Boeing intern				
Daniella Bezuidenhout	ERAU	MS student	2	N	Y, SAFR, BOT
	Prop BB self noise - CHARM, UCD Quietfly				
Vadim Voropayv	ERAU	PhD student	0	N	N
	High prop sims with dist OpenFOAM				
Seyyed Salehian	TU	Asst. Prof.	0.25	N	N
	Co-I; OpenFOAM, CHARM				

Name	Organization	Rank	Salary mo.	For. Collab	For. Travel
W. Nathan Alexander	VT	Assoc. Prof.	1	N	N
	Co-I: experiments				
Nanya Interatep	VT	Assoc. Res. Prof.	1	N	Y FRAN, THAI
	Co-I: experiments				
Szu-Fu Huang	VT	PhD student	12	N	Y, TWAN, JPN
	Co-I: experiments disturbance design				
Shreyas Satish	VT	PhD student	12	N	Y, IMD
	Co-I: experiments PIV				
ThanhLong Duong	VT	MS student	12	N	N
	Experiments, mutlirotor design				
Ryan Lundquist	VT	MS student	4	N	N
	Experiments, BEMT				
Jeremy Bain	JA	Engineer	0	N	N
	Co-I: Industry mentor				
Austin Thai	JA	Engineer	0	N	N
	Industry mentor, Intern director				
Lanju Mei	UMES	Assoc. Prof.	0.25	N	Y, CHIN
	Co-I: Educational partner				

- Boston University (BU)
- Embry Riddle University (ERAU)
- Tuskegee University (TU)
- Virginia Polytechnic Institute and State University (VT)
- Joby Aviation (JA): Jeremy Bain, Austin Thai
- University of Maryland Eastern Shores (UMES)

Co-I S. Salehian of Tuskegee left the instituation on July 14, 2025 for a position at Cadence, Inc.

The following undergraduates participated on the project on an hourly or volunteer basis: David Gardner, Mei Cable, Elliot Dy, Charles Corbett, Sophia Becken, Elliot Macrae-Sadek, Renato Korzinek, Kent Liao. Olivia Virgin was an undergraduate researcher at Tuskegee.

Contents

Executive Summary 1

Major goals and objectives 1

Overview of accomplishments by technical challenge 1

Products 2

Impact 3

Participants and other collaborating organizations 3

Accomplishments 7

1 Urban Disturbances 7
- 1.1 Detailed urban modeling . . . 7
- 1.2 Urban flow parameter study . . . 8
- 1.3 Realistic urban modeling . . . 8
- 1.4 Disturbance characterization and modeling . . . 9
- 1.5 Disturbance coupling to rotor simulations . . . 10

2 Experimental UAM studies 15
- 2.1 Selection of propeller geometry and baseline experiments . . . 15
- 2.2 Characterization and matching of disturbance generator flow . . . 15
- 2.3 SWT measurements of single rotors subject to disturbances . . . 15
- 2.4 SWT measurements of multirotor configurations with different trim conditions - Continued into Year 3 . . . 17
- 2.5 SWT measurements of multirotor vehicles subject to disturbances - Planned for Year 3 18

3 Computational UAM studies 20
- 3.1 Validation of high fidelity simulations . . . 20
- 3.2 Verification and validation of mid and low fidelity simulations . . . 20
  - 3.2.1 Broadband Modeling . . . 23
- 3.3 Simulation of disturbance interaction with multirotors . . . 23

4 Multirotor trim prediction 25
- 4.1 Trim in unsteady setting - Planned for Year 3 . . . 25
- 4.2 Controller for trim optimization given multiple DOF . . . 25

5 Safe trajectory planning for UAM 25
- 5.1 Path planning algorithm . . . 26
- 5.2 Path planning with and without urban flow - Planned for Year 3 . . . 27

Education/workforce development 28

Accomplishments

At the core of this research is the development of accurate methods to predict how rotor performance and noise are impacted by the ingestion of large-scale disturbances that exist due to the urban environment. There were five main areas of focus put forward in the proposal each having a number of subtasks

- Urban flow modeling
- Experimental UAM studies
- Computational UAM studies
- Multirotor trim
- Trajectory planning

Grouping the last two under the umbrella of controls, the interaction of the tasks is visualized in Fig. 1. The accomplishments during the second year in each of these research areas is discussed in

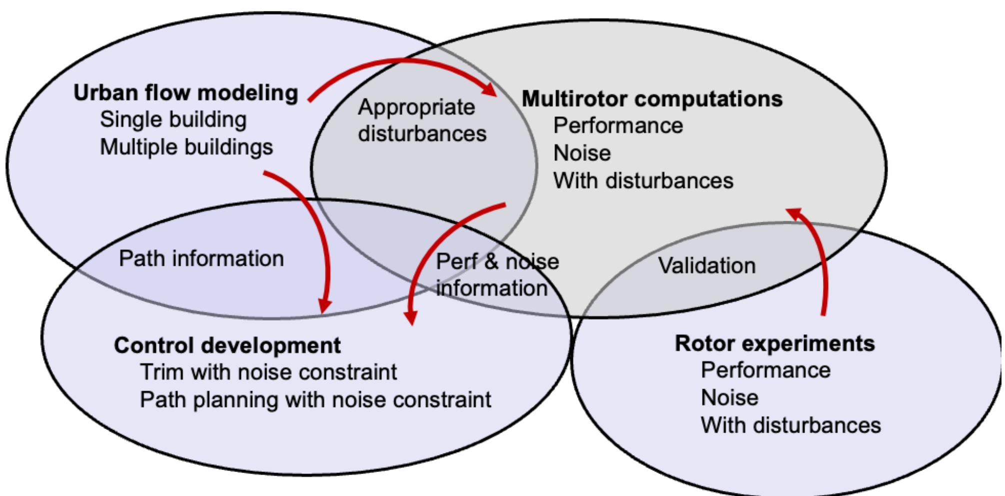

Figure 1: Project diagram with interrelated tasks.

detail in this report. The milestone and gantt charts for each area are reproduced from the original proposal, so that progress can be easily noted.

1 Urban Disturbances

Multirotor vehicles operating in urban settings are expected to take-off and land at vertiports located near buildings and thus will fly through the complex interstitial flows between buildings. As such, understanding better the flow field near buildings and how these change and how they relate to a multirotor vehicle is of interest. Five subtasks provide the framework for our work on urban flow modeling and disturbance characterization. Progress on each is described below.

1.1 Detailed urban modeling

In the first year, OpenFOAM LES and PALM LES were verified against each other. In the second year, the effect of Reynolds number on single building flow outcomes was investigated. Both PALM and OpenFOAM showed that Reynolds number did not affect the main flow disturbance characteristics near a single building. Reynolds number changes were produced by scaling the validation building geometry from wind tunnel size to real building size. Reynolds number changes were also produced by varying the wind speed. Wind speed variation had a larger impact on the results but still the flows seem basically Reynolds number independent in terms of the distrubance behavior near the top of the building (where a vertiport would be located).

The effect of turbulence in the inflow to a building was also studied. Both atmospheric laminar boundary layer flow and turbulent boundary layer flow was specified upstream of a building. It was shown that upstream turbulence decreases the amplitude of the secondary vortex that is shed from the leading edge of the top of the building. But it did not affect any of the flow characterstics downstream of the building.

1.2 Urban flow parameter study

Multiple building configurations were also considered in year two. A continuation of the aligned and staggered canonical building simulations provided turbulence levels near the different buildings in the matrix.

A two-building model, Fig. 2, with the taller building placed upstream, highlights the very different flows at the tops of the two buildings as shown in Fig. 3. The turbulence lengh scale was also studied. It highlights the vortex shedding that takes place at the front edge of the forward building and otherwise shows a general coherence length of about 12% of the building width. The coherent structures at 2.5 m above the buildings are anisotropic with the vertical length scale larger than the streamwise lengthscale. The coherent structures are isotropic within the canopy.

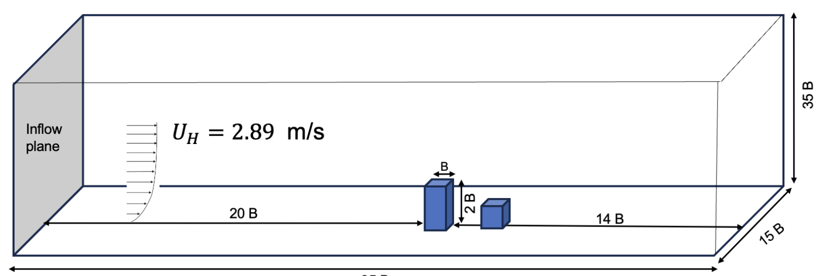

Figure 2: The two building configuration.

The effect of stratification was also considered in a preliminary way. When heating is allowed along surfaces of two buildings and the ground between the buildings, circulating cells between the buildings and a thermal boundary layer above the building form. These affect the local flow conditions. The influence of heating will be studied further in year 3.

1.3 Realistic urban modeling

PALM was used to complete an urban flow simulation for Boston. The Boston building configuration was available from 2018. Increasing resolution was run to get to 1m resolution near the two buildings that were identified as potential vertiports as shown in Fig. 4. The flow field at different times on a given day near one of the buildings is shown in Fig. 5. The time varying flow field was used to obtain a realistic landing condition for a propeller simulation that will be discussed in Section 3.3.

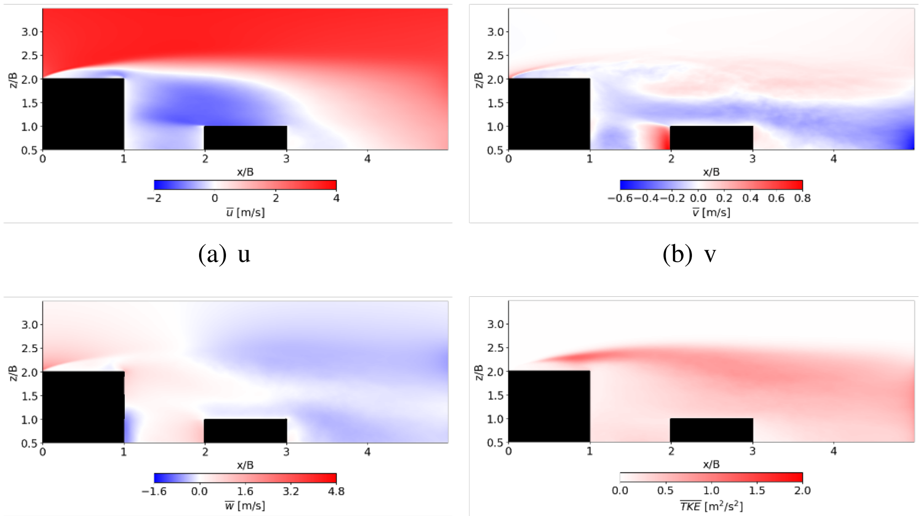

(a) u (b) v

(c) w (d) tke

Figure 3: 2.89 m/s flow past 2 buildings (100m wide, 200 m & 100 m tall).

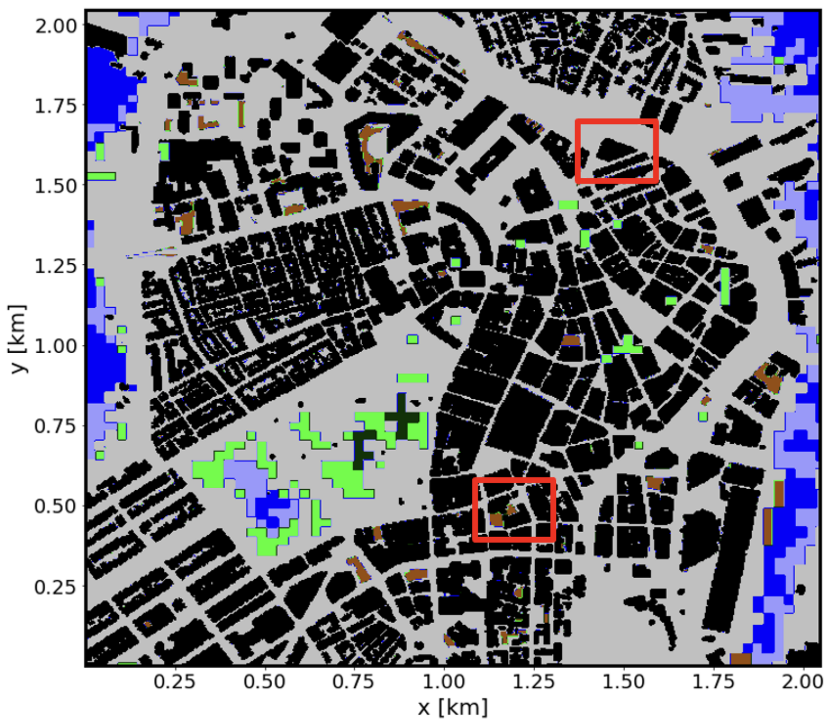

Figure 4: Boston configuration - less resolved simulation region.

1.4 Disturbance characterization and modeling

The SPOD completed in year 1 highlighted various disturbance types in ascending Strouhal number order.

- Base Vortex
- Primary Tip Vortex
- Von Karman Vortex
- Secondary-Tip Vortex

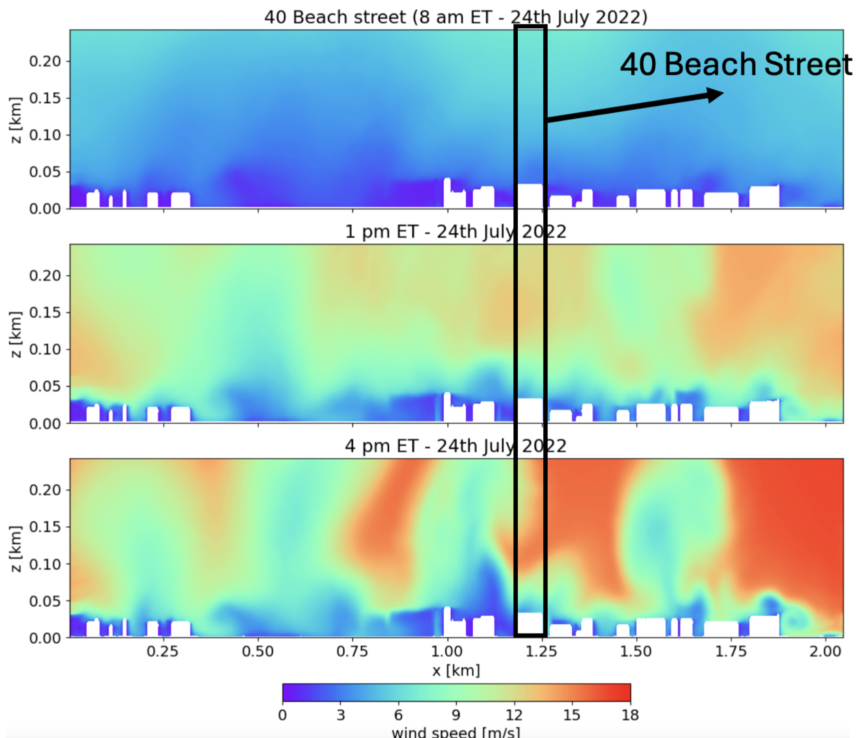

Figure 5: Flow field at different times of the day near the Beech St building.

These were shown to be affected by building arrangement, but remain the main large-scale disturbances. The turbulence levels were also characterized near a building as discussed above. No further breakdown of the disturbance types was performed in year 2.

1.5 Disturbance coupling to rotor simulations

Two main simulation types were run: the Joby prop with the flapped wing upstream; the Joby prop with urban simulation based disturbances.

Both axial and edgewise configurations for the Joby downstream of the flapped airfoil were run. The airfoil is a NACA 0021 to match the experimental setup. The scaled Joby prop was run. A 0 to 20 deg motion in 40 ms was modeled; however, it was later determined that the experiment would run a bit slower. The propeller operated at 4000 rpm. The axial flow case used a mean flow speed of 10 m/s. OpenFOAM was used and the thrust and torque are shown in Fig. 6. As the disturbance approaches, the thrust increases, then it decreases and settles back to the predisturbance value. Torque reacts in the opposite sense. This follows the fact that the disturbance decreases the axial velocity and then increases it which would create the increase followed by decrease in thrust.

The same flapped airfoil disturbance is then simulated with the Joby propeller edgewise to the flow, Fig. 7. Again the mean flow is 10m/s. Now the effect of the flap is more to change the angle of the attack of the flow. It reduces the angle of attack first and then increases it giving a reduction in thrust first followed by a slight increase.

The noise predicted at a mic in the field for both cases as compared to the experimental value for the case without the flapped airfoil disturbance is shown in Fig. 8. In the axial flow case, the disturbance increases the noise slightly. When a spectrum is obtained based on the entire time extent, only a slight increase is seen. However, considering a spectogram of the results shows the instantaneous change to the frequency spectrum as the disturbance interacts with the propeller. The

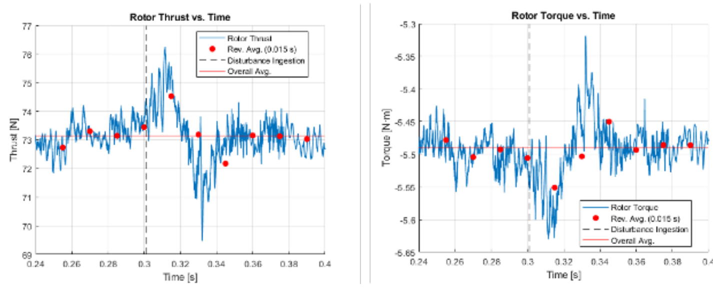

Figure 6: OpenFOAM thrust and torque for Joby at 4000 rpm, flow 10 m/s axial flow with flapped wing upstream.

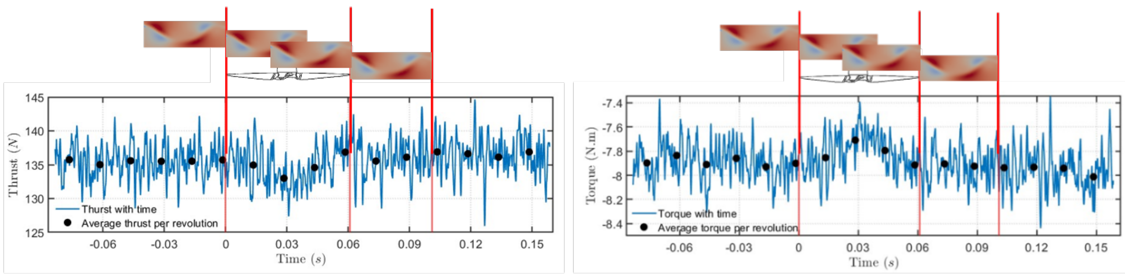

Figure 7: OpenFOAM thrust and torque for Joby at 4000 rpm, flow 10 m/s edgewise flow with flapped wing upstream.

same is true for the edgewise case with even less noise variation seen when the spectrum is obtained from the entire time series.

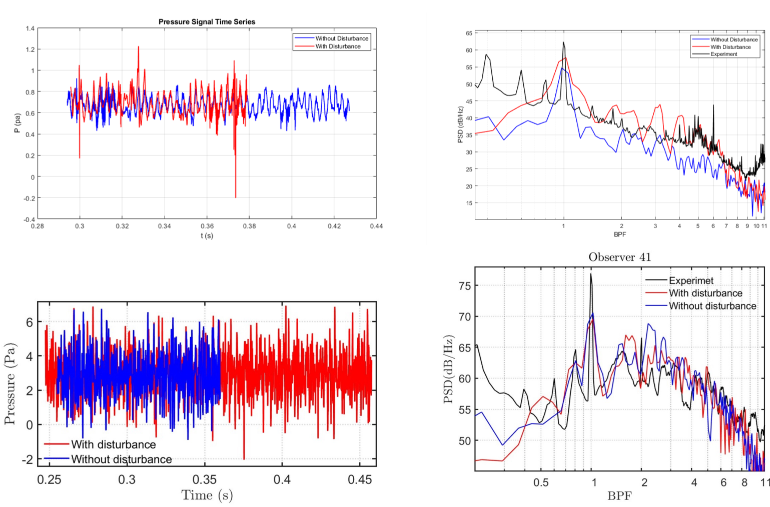

Figure 8: OpenFOAM noise for Joby at 4000 rpm, flow 10 m/s axial (top) and edgewise (bottom) flow with and without flapped airfoil disturbance.

A second set of simulations addressed a slightly different interaction between propellers and disturbances. In one simulation, the Joby scaled propeller was placed in a sinusoidally disturbed flow field as in Fig. 9. The sinusoid altered the flow field perpendicular to the propeller plane. The mean flow was edgewise and carries the disturbance towards the propeller. The propeller's flow field modified the disturbance as it approaches. The disturbance changes the local flow field slightly. Disturbance amplitudes of 10, 20 and 30% of the freestream flow were tested. However, as this is a short wavelength disturbance as compared to the propeller radius, the overall impact on thrust and noise is negligible. The simulations show that the performance and noise is dominated by the propellers interaction with its own wake and that the near wake is not significantly perturbed by this disturbance. It is clear from this test that higher frequency turbulent disturbances should not greatly affect the performance and tonal noise of the propeller. More effort will be needed to quantify the impact on the broadband noise.

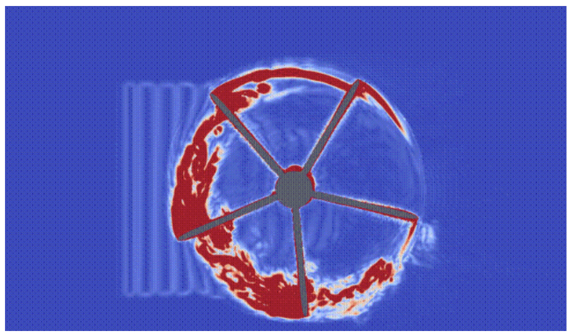

Figure 9: OpenFOAM simulation with sinusoidal disturbance injected as source term upstream of the propeller.

Finally, the influence of a realistic urban flow on the noise from a propeller was considered. The Boston Beech St. vertiport flow field obtained from PALM provided the realistic flow. A landing trajectory based on FAA vertiport rules for an 8:1 approach path was set. The flow field was probed along this path over a time that corresponded to an approach speed of 22 m/s. The flow field obtained for one starting time is shown in Fig. 10. The z-component (flow direction perpendicular to the propeller plane) of the flow field when starting at different times is also shown in the figure. The RMS values for the velocity components over the entire flight path no matter what initial time is used are all relatively the same. As such, any of them can be used to obtain a rough estimation of the effect on the propeller. Simulations were carried out using the mid-fidelity solver ROAM which is part of the Create-AV^{TM} Helios suite. It utlizes an actuator line model and an XFOIL based airfoil table was referenced. Off body, it uses an SA DES for the flow field. The acoustic field was processed using PSU-WOPWOP based on the compact loading vectors. The OASPL at a mic 10 radii away from the propeller was shifted backwards in time and is plotted together with the disturbance flow in Fig. 11. The correlation is clear. It is also clear that the flcutation in the direction perpendicular to the propeller plane is most important. Even though the variations in the flow direction are larger, they do not impact the noise strongly. Methods for parameterizing/capturing the noise difference in a way that can be used in path planning is of interest now.

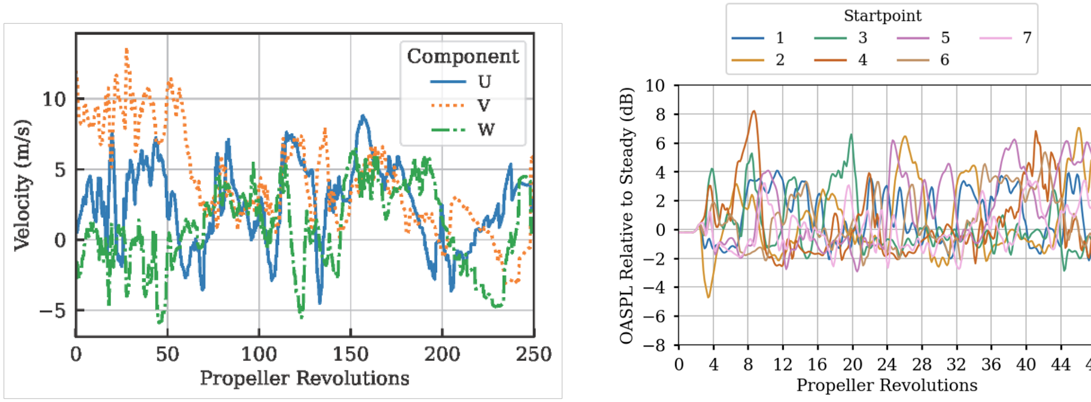

Figure 10: PALM probed flow along descent path in time. Top: 3 velocity components. Bottom: z-component with different starting times.

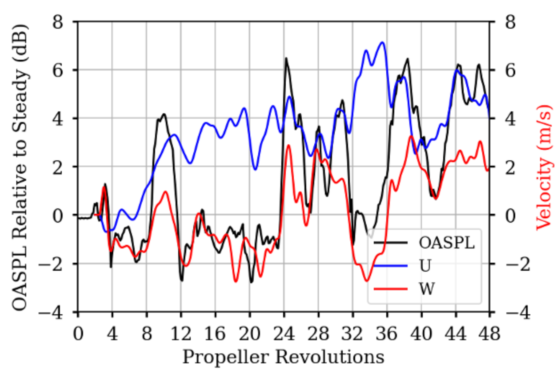

Figure 11: ROAM plus PSU-WOPWOP simulation of noise at mic 10R below the propeller during descent through the disturbed flow.

The urban flow simulation task is hitting its milestones. The simulation methods have been validated and verified; disturbance types of interest near buildings have been identified; the effect of some parameters such as Reynolds number and atmospheric turbulence levels have been quantified; preliminary study of the effect of stratification (thermal loading) has begun; extraction of realistic flows for use with propeller simulations has been demostrated. Development of the urban flow disturbance database now becomes a focus.

Table 1: Milestones and Deliverables for Task 1

Milestone/Subtask /TC/Start-End	**Description (Dependency)**	**Exit Criteria**	**Deliverables**
M1.1/Task 1.1 TC 1/ Q1-4	Detailed urban modeling	Validated urban benchmark completed at high resolution	Simplified urban model configuration (grid), test results, documentation
M1.2/Task 1.2 TC 1,3/Q3-8	Urban flow parameter study (M1.1)	Verification of trends based on wind speed and direction; building config.; stratification	Database of urban simulations for different conditions, documentation
M1.3/Task 1.3 TC 1,2,3/Q9-12	Realistic urban modeling (M1.1,2)	Complete Boston based simulation with 0.1m resolution	Boston flow simulation results (grid, output files) Documentation
M1.4/Task 1.4 TC 1 /Q1-12	Disturbance characterization & modeling (M1.1,2;M2.1)	Disturbances from sims and experiment mapped onto canonical disturbances, scaling	Weighted listing of disturbance types and relevant parameters for describing urban flows
M1.5/Task 1.5 TC 1,2,3/ Q2-5	Disturbances coupled to rotor simulations (M1.4;M3.1,2)	Successful demonstration of stable runs	Example response of rotor to canonical disturbances, documentation of coupling methods

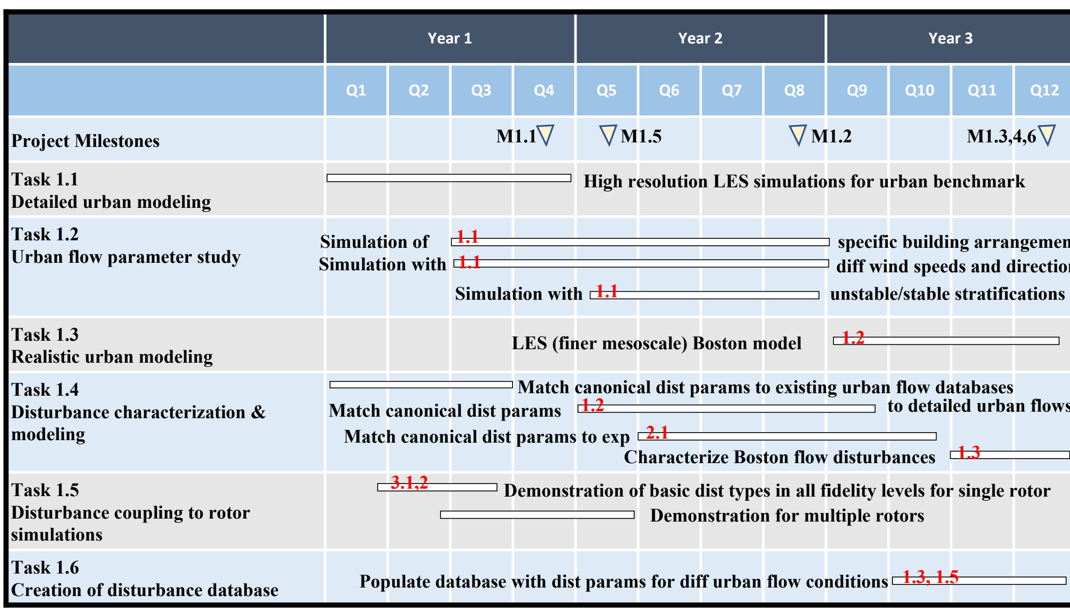

Figure 12: Task 1 schedule. Red indicates required tasks.

2 Experimental UAM studies

Significant progress has been made experimentally in this research program.

2.1 Selection of propeller geometry and baseline experiments

The first subtast was completed in year 1. Year 2 included an effort to scan the blade and make the blade geometry and first round test data available to the larger community. BEMT simulations were run to obtain basic performance parameters for the cases tested in the stability wind tunnel. Comparisons to the experimental data added confidence as the simulations tracked the experiments rather well.

2.2 Characterization and matching of disturbance generator flow

The disturbance generator was fabricated and tested. The NACA 0021 airfoil has a span of 1.83 m with a chord length of 0.15 m and is constructed using carbon fiber sheet layups over a foam core. The carbon fiber skin has a total thickness of 0.2 mm, comprising two layers of 0.1 mm carbon fiber sheets bonded with epoxy. The actuation of a 20° motion is done at 150°/s and 350°/s. It was installed in the Subsonic Modular Anechoic Research Tunnel (SMART) at Virginia Tech and the flow field was captured before, during and after activation using stereoscopic PIV.

Fig. 13 shows the phase-averaged mean flow velocity magnitudes (Fig. 13(a)), flow angles (Fig. 13(b)), and the variances of $\langle U \rangle$ and $\langle V \rangle$ ((Fig. 13(c)&(d)) of the disturbance generated by the 350°/s, 20° flap motion at U_∞= 10 m/s, computed with data from 33 actuations. The analysis presented here focuses on X/D= 0, plotted as a function of non-dimensional time normalized by the freestream velocity and the propeller diameter. During actuation, the shear layer at the top of the open jet is pulled into the field of view (FOV). Therefore, a mask has been applied over this region, as it is not an intended feature of the transient wake and remains beyond the diameter of the propeller.

Prior to $U_\infty \tau/D$ = 2.9, the flow is in its quiescent state. After $U_\infty \tau/D$ = 2.9, the pitch down motion creates a disturbance that spans across the entire height of the FOV. Between $U_\infty \tau/D$ 10 and 13, $\langle U_{mag}/U_\infty \rangle$ experienced a magnitude decrease by 13%, the largest change within the disturbance. Two more phases of the flow are seen before and after $\langle U_{mag}/U_\infty \rangle$ as flow returns to a more settled state.

Deeper analysis of the flow field and comparisons between the flow field behind the flap at the two different actuate rates has been completed.

2.3 SWT measurements of single rotors subject to disturbances

An APC Sport 9×6-4 propeller was placed downstream of the disturbance generator. It is 4-bladed, 0.23 m in diameter, and has a 0.15 m pitch. The propeller is coupled with a T-Motor AT2820 KV1250 motor, which measures 35.2 mm in diameter and 63.5 mm in length, including the shaft. An additional shaft attachment, included with the AT2820 package, is used on the rear end of the motor, which extends the total length to 91.5 mm. The propeller is mounted to this additional shaft attachment via an included nut. The recommended TMotor AT75A electronic speed controller (ESC) is used in conjunction with an Arduino Uno Rev 3 to control the rotational speed of the motor.

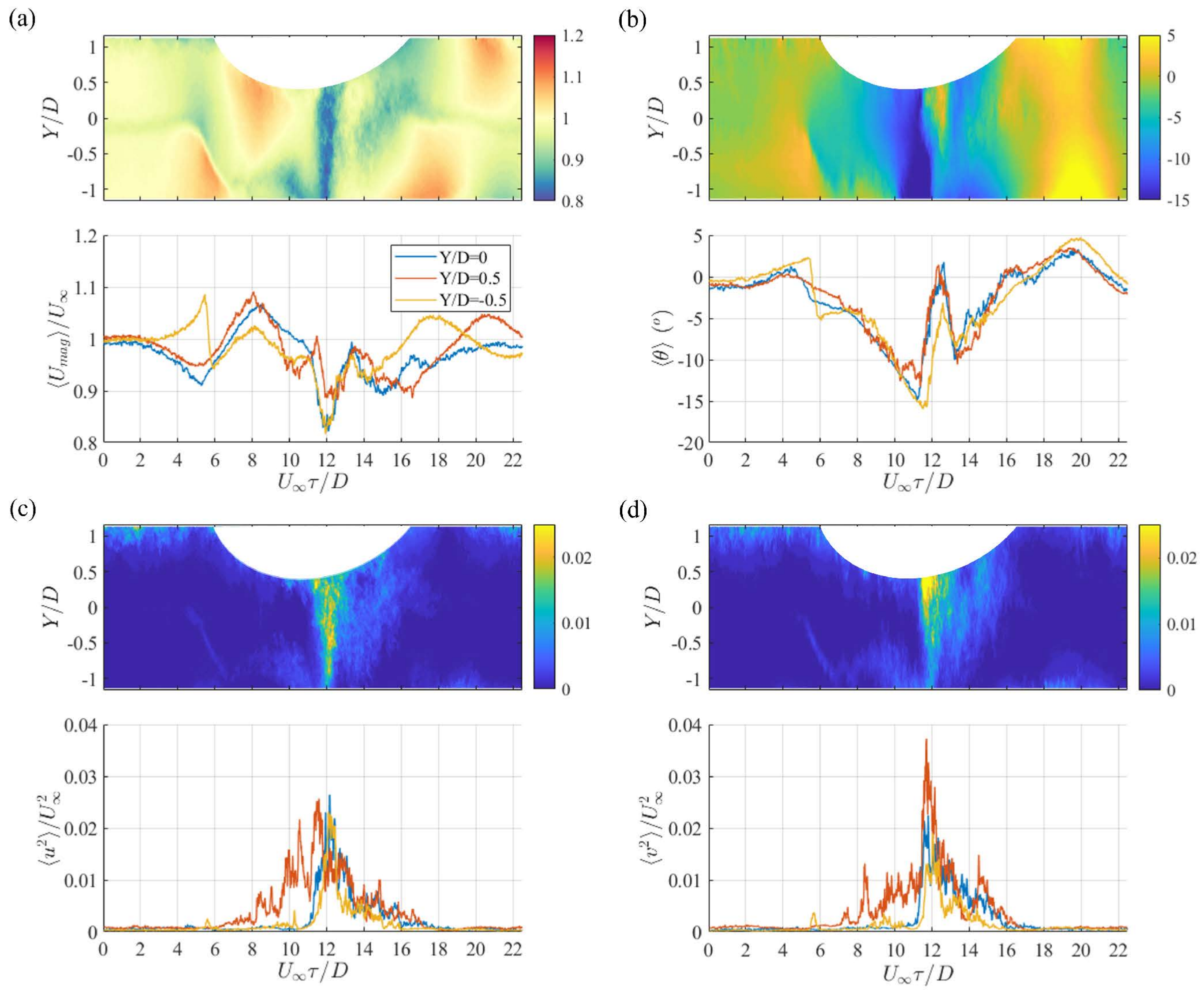

Figure 13: (a) $\langle U\rangle/U_\infty$, (b) $\langle\theta\rangle$ in degree, (c) $\langle u^2\rangle/U_\infty^2$, and (d) $\langle v^2\rangle/U_\infty^2$ of the 350°/s, flap with $\alpha = 20°$ at U_∞= 10 m/s.

The speed of the motor was measured with a laser diode. The propeller was tested at 4000, 5000, and 6000 RPM with a freestream velocity of 10m/s, corresponding to advance ratios μ of 0.21, 0.17, and 0.14, respectively.

Noise measurements were made using an array of six microphones mounted on the ceiling of the test section. The microphones used for the measurements are Bruel & Kjaer 1/2" type 4190 microphones. They have a dynamic range of 15-146 dB and a sensitivity, measured at 250 Hz, of -26 dB $\pm$1.5 dB re 1 V/Pa within a 6.5-20 kHz frequency range. Data were acquired at 65536 Hz for a duration of 32 s using Bruel & Kjaer Type 3050 modules. The microphones were positioned vertically 0.9 m from the center of the propeller disk and offset by 0.01 m in the positive Z-direction relative to the propeller's axis of rotation. The microphones were arranged to form an array that samples a range of observer angles between -30° and 45°, with an interval of 15°.

The results when the propeller is at 6000 rpm and the flap is actuated at 350°/s with flap angle 20° are shown in Fig. 14. Figure 11 presents the total spectrograms of the propeller ingesting a transient disturbance averaged over 195 actuations in both axial (Fig. 14(b)) and edgewise (Fig. 14(c)) configurations. The figure represents the spectrogram observed by a single microphone,

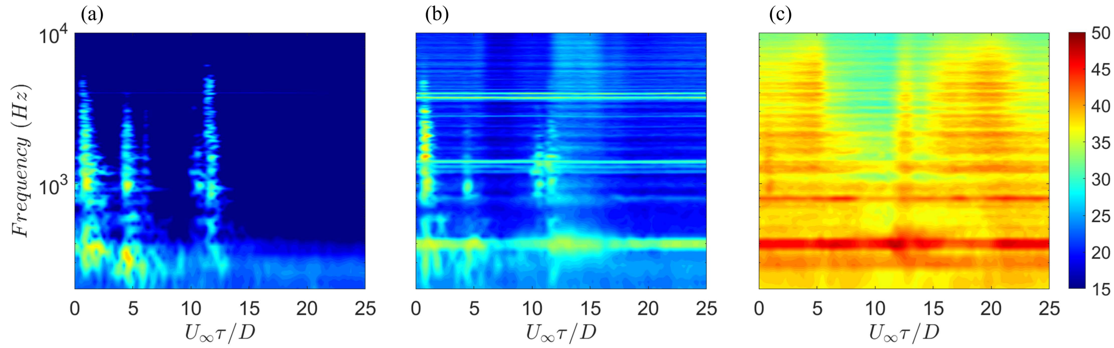

Figure 14: Spectrogram of the propeller ingesting at 20°, flap disturbance actuated at 350°/s and operating at μ = 0.14: (a) actuation background noise (no propeller), (b) axial configuration, and (c) edgewise configuration.

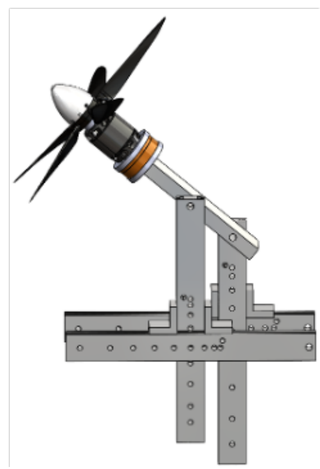

Figure 15: Single prop tile mechanism for multirotor test stand.

which was in the plane of the propeller disk. The contours in the figure indicate PSD in dB/Hz. Fig. 14(a) shows the actuator background noise in the absence of the propeller stand. The effect of the disturbance, in particular the gradients of the flow field from the flap motion, are evident in the figures. The results were analyzed further by separating the deterministic and probablistic components of the noise signals. A key observation from both the axial and edgewise configurations is that the majority of the disturbance-induced response is captured in the probabilistic component, underscoring the broadband and non-deterministic nature of the gust interaction. However, in the edgewise configuration, the deterministic component appears less affected by the gust interaction. These overarching results all support the findings from the computations of the different disturbance types interacting with a propeller.

2.4 SWT measurements of multirotor configurations with different trim conditions - Continued into Year 3

The multirotor platform has gone through one design cycle as seen in Fig. 15. Currently the aerodynamic design of the individual tilt mechanism is being improved. The motor has been selected : TMotor AT2820 KV1250. The initial force measurement device, 6-component,ATI Nano43 SI-36-0.5 load cell, forces up to 36N, moments up to 0.5Nm was damaged during the VTSMART test and determined to be not robust enough. A new load cell is being sourced.

2.5 SWT measurements of multirotor vehicles subject to disturbances - Planned for Year 3

Task 2 is slightly behind due to the renovations of the stability wind tunnel (SWT). However, VT was able to add the experimental test of the APC prop behind the disturbance providing insight into the general behavior of such a configuration. This fall, the single Joby propeller ingesting the flapped wing disturbance will be tested in the SWT. This will put the task back on track.

Experimental results for the Joby propeller in various flow conditions have been made available to the larger community. The findings differ from those taken elsewhere and as such NASA will perform an additional experiment using our exact model geometry. This will nail down if differences are due to test chamber differences. Preliminary propeller-disturbance performance and noise data is now available for a small propeller. The disturbance flow field is well characterized. This Task is slightly behind due to the renovations of the stability wind tunnel (SWT) but will be caught up this fall when the Joby propeller is placed behind the disturbance in the SWT. The multirotor platform is almost fully designed and will also be deployed in year 3.

Table 2: Milestones and Deliverables for Task 2

Milestone/Subtask /TC/Start-End	**Description (Dependency)**	**Exit Criteria**	**Deliverables**
M2.1/Task 2.1 TC 1,3/ Q1-4	Characterization & matching of disturbance generator flow (M1.4;M3.1,2,3;M4.1)	Aerodynamic and acoustic measurements of disturbances	Time-resolved data of disturbance for comparison with urban flow simulations and computational models
M2.2/Task 2.2 TC 1,2/Q1-2	Selection of UAM rotor geometry (M3.1,2,3;M4.1)	Agreement on rotor configurations by proposal team and NASA POC	Detailed propeller characteristics necessary for fabrication
M2.3/Task 2.3 TC 1/ Q2-6	SWT perf. and noise measurements of single rotors subject to disturbances (M1.4;M3.1,2)	Acquisition and analysis of perf and noise data for single rotor configurations subject to a family of disturbances	Thrust and torque. Unsteady velocity near the rotor showing interaction with disturbances and noise measurements at multiple observer locations.
M2.4/Task 2.4 TC 2,3/Q3-9	SWT perf and noise measurement of multirotor with diff trim conditions (M4.1)	Acquisition and analysis of perf and noise data for multirotor configurations at diff trim settings	Acoustic measurements and individual rotor perf data as well as unsteady velocity into downstream rotors
M2.5/Task 2.5 TC 1,2/Q8-10	SWT perf and noise measurement of multirotor subject to disturbances (M3.3;M4.1,2)	Acquisition and analysis of perf and noise data for multirotor configurations interacting with a family of disturbances	Unsteady velocity measurements of disturbances as they interact with the rotors and their effect on the rotor wakes as well as noise at multiple observer locations. Individual rotor perf.

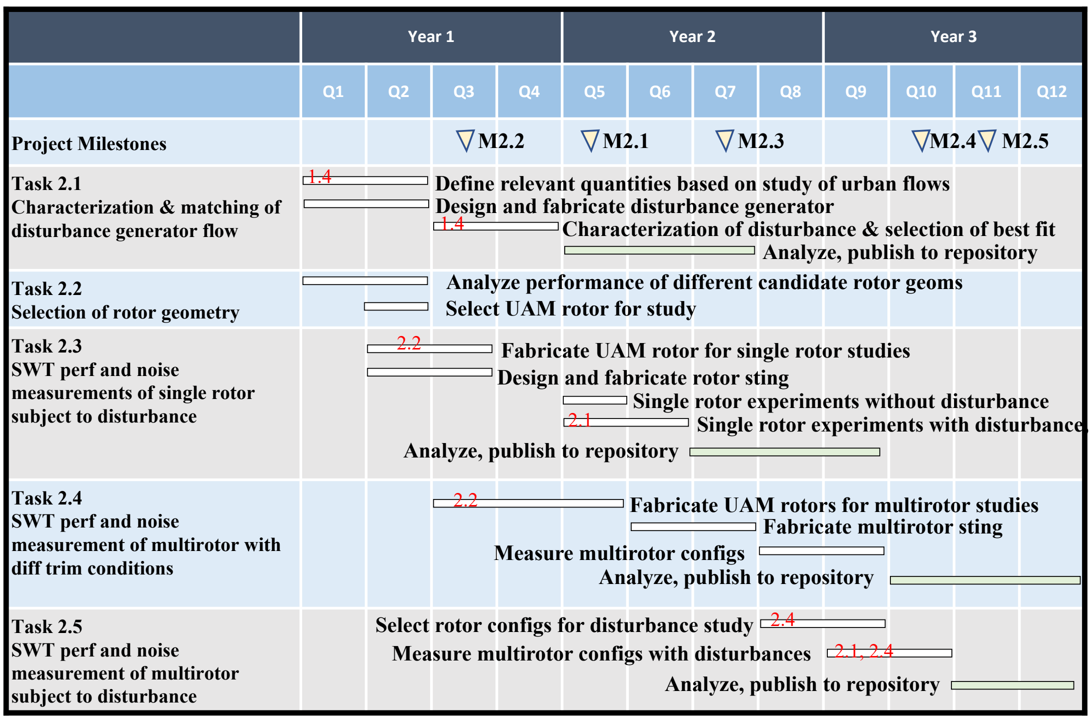

Figure 16: Task 2 schedule. Milestones set at completion of experimental campaigns. Red indicates required tasks.

3 Computational UAM studies

A main focus of this work is accurate computational prediction of multirotor performance and noise. The second year increased our list of best practices for mid and high-fidelity propeller and multirotor simulations.

3.1 Validation of high fidelity simulations

High fidelity simulations of the single Joby propeller at several operating conditions were completed. OpenFOAM, Helios and overflow all predict too low of thrust and do not agree with each other. The source of the discrepancy is still not well understood and we continue to investigate.

Further investigation was made into the prediction of noise from propellers using impermeable and permeable FWH methods. OpenFOAM can now be coupled to PSU-WOPWOP, so the FWH methodology is now consistent across all computational platforms we are using. Different end cap treatments for the permeable surface were tested with both OpenFOAM and Helios simulations. A best end-cap averaging method has not yet been determined.

As vertiport modeling requires the propeller to be acting in the presence of a ground plane, an investigation into how to utilize image propellers properly and/or select the proper permeable FWH surface was completed.

Each of these topics have been described fully in recent conference papers.

3.2 Verification and validation of mid and low fidelity simulations

CHARM has been and continues to be validated against the VT single propeller measurements. It was determined that a normal method for developing airfoil tables from XFOIL was not sufficient. Instead, the airfoil table needs to be created for the exact RPM of interest with each spanwise section being computed at its exact Reynolds number. The thrust results, even with the more accurate airfoil tables, are high at higher RPM. Many of the results are available in the PhD dissertation of M. Marque-Goncalves.

CHARM was also tested more extensively for the SUI quadrotor. The SUI provided a multirotor platform for which there is a trove of performance data and some acoustic data (all from prior NASA tests). After several discussions with the CHARM developers, best settings were determined for running these multirotor simulations. An example performance outcomes is shown in Fig. 17. More results will be reported in a Scitech 2026 paper.

The acoustic predictions were validated against the Langley Low Speed Aeroacoustic Wind Tunnel (LSAWT) test. The above-vehicle microphone set up is shown in Fig. 18. Microphones were deployed below the vehicle as well, also in a linear array but were 3.54 m down from the vehicle.

Hover was tested as well as a forward flight case with the freestream Mach number set to 0.045 which is 15.3 m/s and the vehicle pitched at -10°. There were different target thrust values, here we focus on the 45N case. The rotors were spun at roughly 4700 RPM in hover to achieve this thrust and in the forward flight setting they were set with the forward rotors at 3900 and the reward at 4910 to achieve a trim state, Table **??**.

Spectra at a far-field observer calculated by PSU-WOPWOP using the inputs automatically generated by CHARM can be seen in 19. The signal is calculated from all four propeller loading files simultaneously, which clearly hides some of the tonal peaks when propellers are spinning at different rates, especially ones very close to each other.

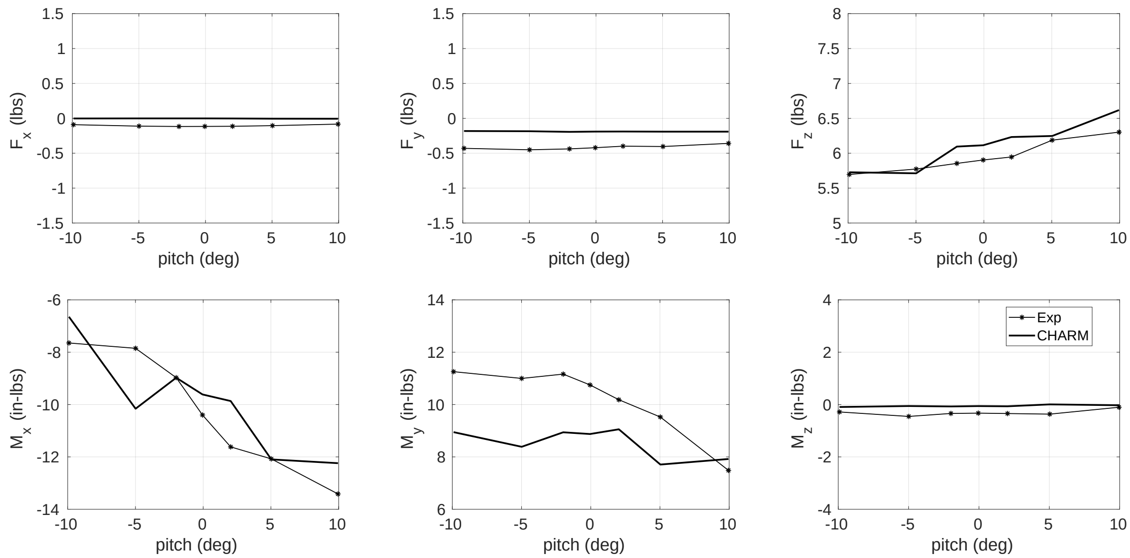

Figure 17: SUI prediction with CHARM vs experiment. Two props at 3800 and two at 3200, Yaw = 90°, varying pitch.

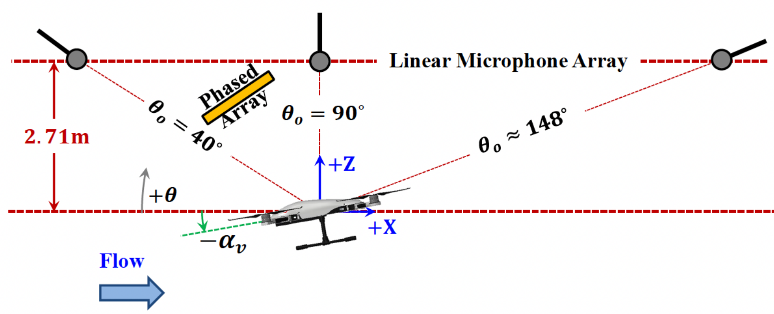

Figure 18: Acoustic measurement setup.

In order to better characterize the signals, a processing scheme was devised that runs a separate PSU-WOPWOP calculation for each propeller at a given observer location. Then, each propeller's time-domain signal can be trimmed to be an integer multiple of its period and multiplied by a Hanning window. These operations will minimize spectral leakage when calculating a FFT, and ensure that each harmonic of the blade passage frequency (BPF) coincides with a frequency bin. After performing the FFT, the complex amplitude of each BPF harmonic can be extracted. Once the amplitudes of each propeller's BPF harmonics have been calculated, the signals can be reconstructed in the time domain for a longer period, e.g. 10 times the maximum propeller period, and added in the time domain. Increasing the signal length will allow a finer frequency resolution, so that when an FFT is applied to the summed reconstructed signal, the BPF tones of each propeller are revealed

Table 3: Propeller speeds to achieve desired trim for the SUI forward flight case.

	Rotor 1	Rotor 2	Rotor 3	Rotor 4
Exp.	4075	3992	4895	4937
CHARM (MREV)	3900	3900	4910	4910

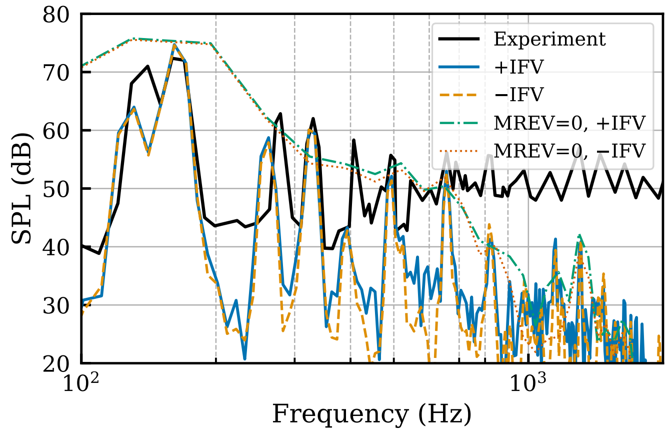

Figure 19: Unprocessed PSU-WOPWOP solution of CHARM's generated input files. Experimental results from Zawodny, 2022.

more clearly.

The acoustics for this case are shown in Fig. 20. Fig. 20(a) shows the spectra at a microphone above and to the side of the drone in a forward flight configuration from Zawodny's 2022 experiment. Fig. 20(b) shows the spectra at a microphone in front and below the drone at in a forward flight configuration from Zawodny's 2018 paper. In the reference frame shown in Fig. 18, these microphones are located at [0.0, 2.278, 2.71] and [-1.288, 0.0, -3.54], respectively. Fig. 20(c) shows the spectra at the same location but in a hover condition. The tones are much clearer when using the new processing technique.

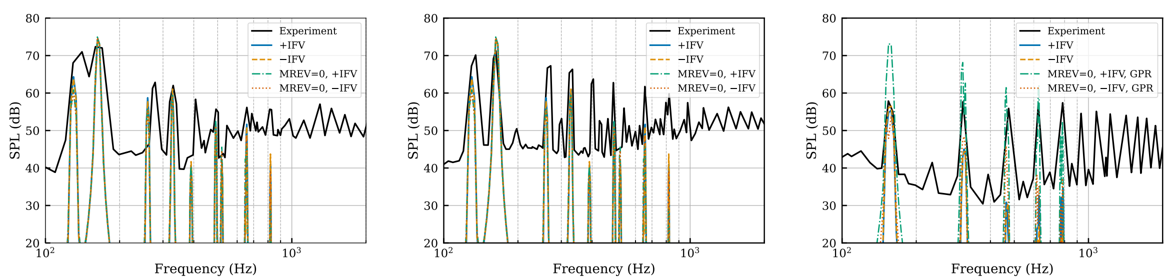

(a) Mic at 90° above (b) Mic at 70° below (c) Mic at 70° below

Figure 20: SPL for forward flight (a) & (b) and hover (c).

ROAM was also tested for mid-fidelity simulations. The results from the validation against the Joby propeller experiments wasn't great and will be addressed further in the future. Still, ROAM was used to compare results for with and without disturbances. It was verified that the component of the disturbance perpendicular to the plane plays the largest role. As well, the disturbance contributes additional broadband noise and slightly modifies the tonal amplitudes. ROAM will be further vetted in year 3.

Other methods were also considered in year 2. VSPAERO, FLOWUnsteady and DUST were all preliminaryly tested. VSPAERO could not connect easily to PSU-WOPWOP and as such was not fully utilized. FLOWUnsteady was obtained and run on example cases but not applied to the Joby propeller yet. DUST was utilized to compute the Joby propeller in axial and edgewise flight. The performance values differed from the experimental values by 3% for axial and 10% for edgewise.

It was determined that the wake structure compares favorably between DUST and high-fidelity solutions. Further efforts to improve the simulations will take place in year 3. DUST is currently being coupled to PSU-WOPWOP and the noise predictions will be evaluated. DUST is of interest because others have shown it can handle inflow disturbances well. It is also open source which has benefits as compared to CHARM.

3.2.1 Broadband Modeling

Year 2 had a focus on applying the existing UCD-Quietfly for trailing edge broadband noise to the Joby CHARM simulations. These were reported in the PhD thesis of Marques-Goncalves. UCD-Quietfly is also being used to investigate the trailing edge broadband noise associated with the AART which has been simulated using Helios. These results will be reported in an upcoming journal paper.

3.3 Simulation of disturbance interaction with multirotors

This was described in detailed in Section 1.5.

The computations provided a better understanding of the limitations of the permeable FHW method when applied to propeller flows. It was demonstrated that reasonable acoustic directivity patterns can be obtained using high-fidelity simulations for the Joby propeller as compared to the experiments. The open source high fidelity tool was shown to give reasonable accuracy and a converter so that its output can be coupled to PSU-WOPWOP was created. The mid-fidelity tool CHARM was shown to work well for both the Joby propeller and the mutirotor SUI configuration. A new processing method for the acoustics was created for the multirotor application which enables better resolution of the multiple tones.
Currently, the high-fidelity simulations for multirotors is lagging. There is previous work that has addressed the application of Helios to the SUI configuration that is being used to address this gap. At the beginning of year 3, we will identify how the multirotor simulations should progress in order to support the overarching goals of the project. For year 3, new broadband noise modeling will take place. The focus will be leading edge broadband noise. This is necessary as it has become clear that ROAM and CHARM must be utilized more for the multirotor simulations and neither captures any broadband noise.

Table 4: Milestones and Deliverables for Task 3

Milestone/Subtask /TC/Start-End	Description (Dependency)	Exit Criteria	Deliverables
M3.1/Task 3.1 TC 1,2,3/Q1-5	Validation of high fidelity (M2.3)	Performance to within 5% and noise to within 3dB for tonal and 3 dB OASPL compared to data	Validation test cases and simulation results
M3.2/Task 3.2 TC 1,2,3/Q1-9	Validation of mid and low fidelity (M2.3)	Performance to within 10% and noise to within 3dB for tonal and 3 dB OASPL compared to data	Validation test cases and simulation results
M3.3/Task 3.3 TC 1/Q3-10	Disturbance interaction with multirotors (M1.3,4; M2.4;M3.1,2)	Performance to within 5% and noise to within 3dB for tonal and 3 dB OASPL compared to data	Validation test cases and simulation results

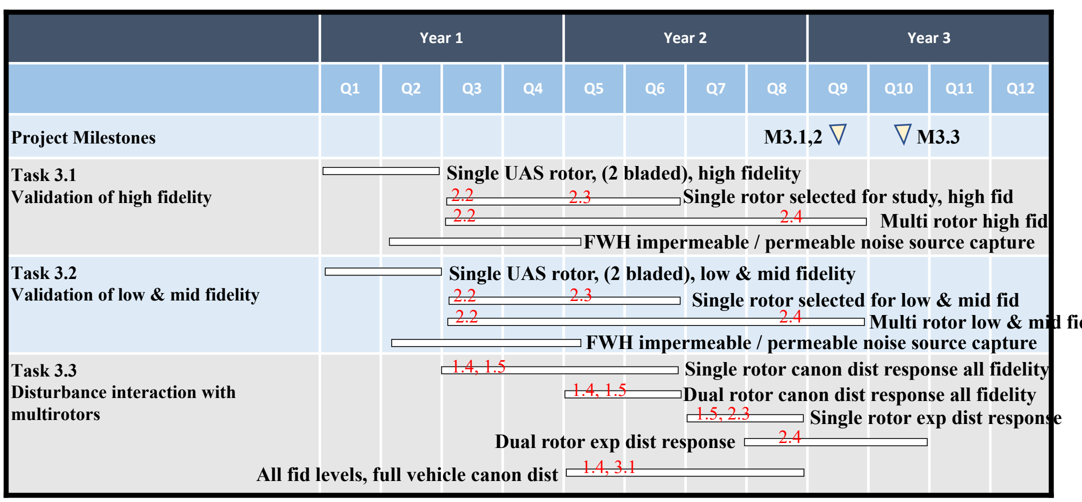

Figure 21: Task 3 schedule. Red indicates required tasks..

4 Multirotor trim prediction

4.1 Trim in unsteady setting - Planned for Year 3

4.2 Controller for trim optimization given multiple DOF

In order to create a trim optimization method that utilizes noise as a metric, a control method for including this new parameter is required. Real-time assessment of the performance and noise of a multirotor vehicle is intractable. Currently, performance values are estimated using simple rules that link propeller location, attitude and rpm to thrust and torque. Such rules have been sought for our example multirotor, the SUI quadrotor. A database of performance values and a sound metric at 3 microphones was created using CHARM. The sound metric that was chosen is a simple summation of the first 10 tones provided as an OASPL$_{tonal}$. A machine learning type method, the Gaussian Process, is used to develop the rules. The parameter space originally identified over 2 million states. This was too large of database for the GP to effectively handle. As such, a latin hypercube method was used to select cases from the 8 dimensional space. 5000 cases were identifed using the latin hypercube method and simulated with CHARM & PSU-WOPWOP.

The GP results indicate good convergence of the rules on the parameter space. These rules are now being used in simulation to test the control of the quadrotor. Tests will reveal how many operating states are possible for completing a simple task such as straight flight with a given heading. From these, a lower noise state will be identified.

An efficient method for developing and utilizing a multirotor performance and noise database to inform control decisions has been developed. It is still being tested for trim control in both simulation and in the lab. Task 4 has not addressed the addition of an updated trim algorithm for high fidelity simulations. This delay is due to the lack of high fidelity simulations that can feed the control algorithm and the need for great amounts of computational resources in order to run the high fidelity simulations. Given the challenges, the controls may only be applied to the mid-fidelity as this project progresses.

Table 5: Milestones and Deliverables for Task 4

Milestone/Subtask /TC/Start-End	**Description (Dependency)**	**Exit Criteria**	**Deliverables**
M4.1/Task 4.1 TC 2,3/ Q3-11	Trim in unsteady setting (M2.4,5;M3.3)	Verification across fidelities. Validation within 2% on RPM and 2° on pitch and associated noise to within 3dB OASPL	Verification tests, Validation tests, Insights into effect of trim inclusion on disturbance response
M4.2/Taks 4.2 TC 2,3 / Q6-9	Trim optimizer based on noise metrics (M2.4;M3.2,3)	Demonstrate trim optimization with multiple DOF	Optimization method with newly defined constraints for multi DOF trim

5 Safe trajectory planning for UAM

While obstacle avoidance and following reference trajectories are common in path planning, the addition of noise as a constraint represents a new challenge in the field. A new path planning method

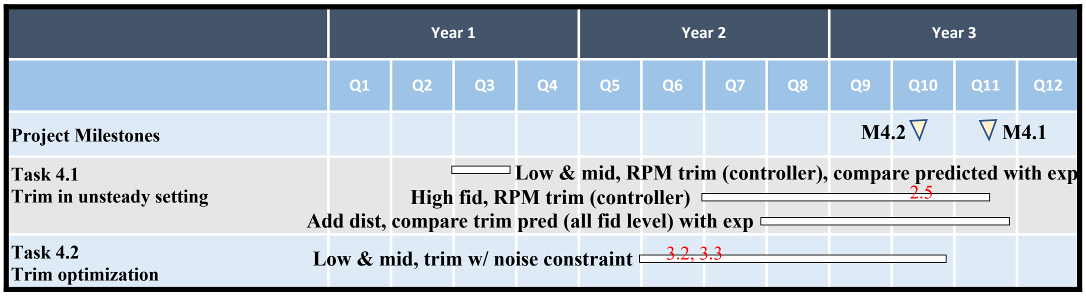

Figure 22: Task 4 schedule. Red indicates required tasks.

is being developed. At first, it is assumed that the multirotor and the buildings exist in a no flow environment.

5.1 Path planning algorithm

In year 2, the RRT* trajectory planning was updated using a Control Barrier Function (CBF). This allows for the noise to be seen better as a constraint. Fig. 23 demonstrates that branches do not exceed the limit of the accumulated noise The final path (red) satisfies the CBF noise constraint while also avoiding obstacles from the start (blue) to the goal (magenta). Two scenarios with different strengths of the CBF criteria lead to different paths.

Two microphones were set up in the lab. The noise of a small Tello drone was measured as a function of distance and fit with a simple curve. This function was used to define the CBF. Simulations for the Tello to move through multiple buildings to the opposite end of the room showed that the drone would have to fly around on a longer path in order to avoid unwanted noise levels at the buildings. Without the noise constraint, a straight path through the middle of two of the buildings would be selected. In the lab in real-time, the Tello chose a path very close to the simulated path as seen in Fig. 24.

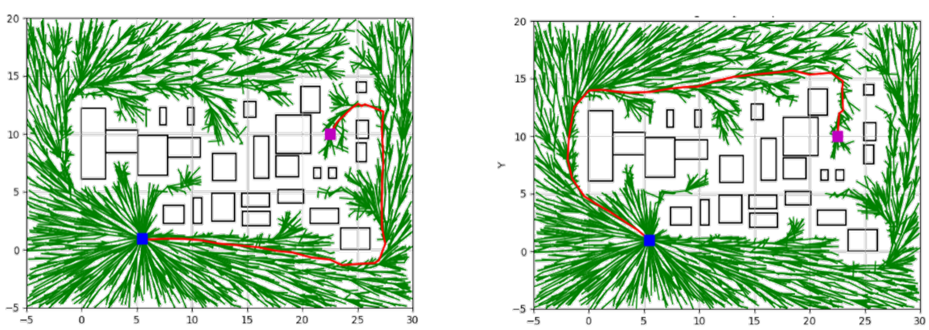

Figure 23: Paths selected due to different strengths of the noise CBF.

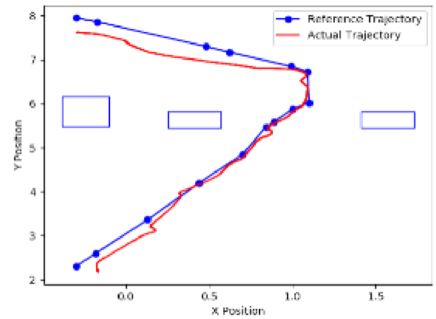

Figure 24: Simulation vs actual drone test in the lab, with noise constraint as part of the controller.

5.2 Path planning with and without urban flow - Planned for Year 3

Path planning for an aerial vehicle that includes noise and obstacle avoidance has been demonstrated in simulation and in the lab with a small quadrotor. At the beginning of year 3, a more complicated model for the vehicle noise based on computed noise spheres will be used to create the CBF. Ray tracing to include the effect of wave reflection off of buildings will also be used to inform the CBF.

Table 6: Milestones and Deliverables for Task 4

Milestone/Subtask /TC/Start-End	**Description (Dependency)**	**Exit Criteria**	**Deliverables**
M5.1/Task 5.1 TC 3/Q5-8	Extend controller (M4.1)	Demonstrate cumulative and area constraints	Improved CLF-CBF algorithm
M5.2/Task 5.2 TC 3/Q4-8	Path planning algorithm (M3.3)	Demonstrate simulation of diff path outcomes due to diff noise constraints	Extended RRT* algorithm
M5.3/Task 5.3 TC 3/Q8-12	Path planning w/ & w/o urban flow (M1.3;M3.3;M4.3)	Demonstrate path planning through Boston model	Simulation results. Method details.

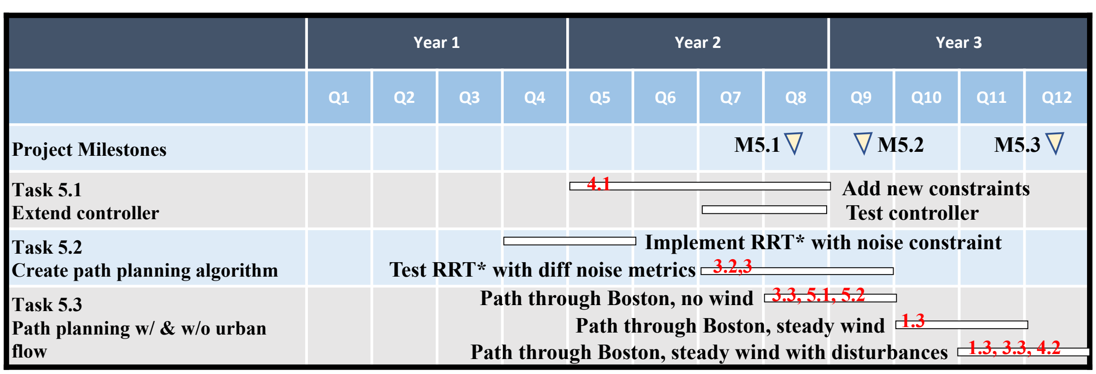

Figure 25: Task 5 schedule. Red indicates required tasks.

Education/workforce development

A workshop was held on the campus of Embry Riddle Aeronautical University May 14-16, 2025. 18 students from across the country attended. These students were rising undergraduate juniors and seniors. Recruitment focused on schools without graduate programs and schools that have a high number of minority students enrolled in ENG. One objective of this program was to highlight the opportunities available for students in graduate school so that they might consider applying to graduate programs. This workshop included some relevant lab tours and a visit to the flight simulators on campus.

Students were led through the process of predicting propeller aerodynamic performance and then they were introduced to the ideas behind predicting noise. In addition, they programmed Tello drones and flew them through an obstacle course. Guest speakers included representatives from Whisper Aero, Joby Aviation, and Blue Ridge Consulting. Fig. 26 shows a picture of the undergraduate participants during their visit to ERAU simulator facility.

Figure 26: Students visiting the simulator facility.

Joby hosted four interns affiliated with the NASA ULI program during the summer of 2025, Fig. 27.

- Elliot Macrae-Sadek (MS, BU) – Rotordynamics Intern. Optimization of loads automatic postprocessing framework
- Daniel Maleev (MS, ERAU) – Computational Fluid Dynamics Intern. NASA OVERFLOW simulations of the Joby aircraft
- Ian Doud (BS, BU) – Aircraft Performance Intern. Hover performance flight test verification and analysis
- Idris Seidu (PhD, BU) – Flight Controls Intern. Evaluation of stability margins and vehicle performance

All the interns took trips to other Joby facilities in San Carlos and Marina, CA. The internships were a valuable experience for the interns. These students will now continue their ULI research which will now be highly informed by their internship experience and their deeper knowledge of the Joby aircraft.

Figure 27: Joby summer 2025 interns. (Left to right) Elliot, Daniel, Ian and Idris.